

In Situ Doping Strategy for the Preparation of Conjugated Triazine Frameworks Displaying Efficient CO₂ Capture Performance

Xiang Zhu,[†] Chengcheng Tian,^{*,†} Gabriel M. Veith,^{||} Carter W. Abney,[‡] Jérémy Dehaudt,[†] and Sheng Dai^{*,†,‡}

[†]Department of Chemistry, University of Tennessee—Knoxville, Knoxville, Tennessee 37996-1600, United States

[‡]Chemical Sciences Division, Oak Ridge National Laboratory, Oak Ridge, Tennessee 37831, United States

^{||}Materials Science and Technology Division, Oak Ridge National Laboratory, Oak Ridge, Tennessee 37831, United States

S Supporting Information

ABSTRACT: An *in situ* doping strategy has been developed for the generation of a novel family of hexaazatriphenylene-based conjugated triazine frameworks (CTFs) for efficient CO₂ capture. The resulting task-specific materials exhibit an exceptionally high CO₂ uptake capacity (up to 4.8 mmol g⁻¹ at 297 K and 1 bar). The synergistic effects of ultrananoporosity and rich N/O codoped CO₂-philic sites bestow the framework with the highest CO₂ adsorption capacity among known porous organic polymers (POPs). This innovative approach not only enables superior CO₂ separation performance but also provides tunable control of surface features on POPs, thereby affording control over bulk material properties. We anticipate this novel strategy will facilitate new possibilities for the rational design and synthesis of nanoporous materials for carbon capture.

The interest in curtailing greenhouse gas emissions through removal of CO₂ from flue gas of coal-fired power plants has inspired an extensive search for novel nanoporous materials capable of efficient physical adsorption of CO₂.^{1–12} Porous organic polymers (POPs), an advanced class of porous materials, have emerged as a possible solution due to their overall stability and the ability to impart desirable functionalities for task-specific applications. Although much progress has been made in assembling multidentate organic building blocks to yield a wide variety of POP-based CO₂ adsorbents,^{13–28} only moderate CO₂-uptake capacities were observed under conditions relevant to industrial carbon capture, where the CO₂ concentration is in the range of 10–15%. This underwhelming performance can largely be attributed to the limited CO₂ affinity of POPs reported thus far. Inducing strong electrostatic interactions between the polarizable CO₂ and the material surface is expected to significantly increase the CO₂ capture performance. Unfortunately, conventional postsynthetic incorporation of CO₂-philic sites into the framework often results in a compromise of porosity of the adsorbent,²⁰ which plays another crucial role on carbon capture. Herein, we report an *in situ* doping strategy to create a novel family of POP-based adsorbents displaying superior adsorption toward CO₂ at low concentrations. The critical development is the preparation of an intrinsic ultrananoporous environment with abundant surface active sites with

high affinity for CO₂ binding. Extensive ultrananoporosity imparts inherent molecular sieving capabilities to provide greater accessibility to CO₂-philic sites, therefore cooperatively enhancing the affinity of the materials for CO₂. This innovative approach not only enables us to achieve an exceptionally high CO₂ uptake for POPs but simultaneously provides a means to control the surface features, thereby tuning the properties of the material.

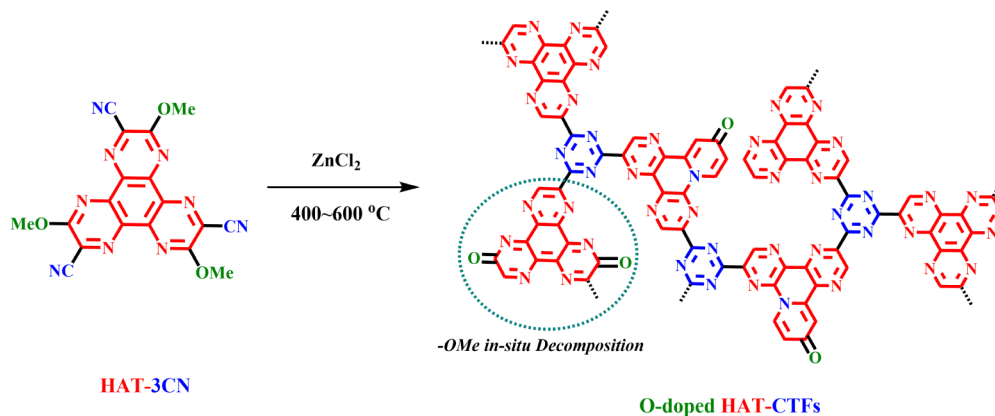
As shown in [Scheme 1](#), we synthesized 3,7,11-trimethoxy-2,6,10-tricyano-1,4,5,8,9,12-hexaazatriphenylene²⁹ (HAT-3CN) as our scaffold for the construction of task-specific conjugated triazine frameworks (CTFs). Among various types of POPs, CTFs possess high stability and excellent porosity in addition to intrinsic N-doping and have emerged as promising candidates for carbon capture.^{30–33} While displaying adequate CO₂ uptake at higher pressures, these reported materials exhibit rather low CO₂ uptake at 0.15 bar (partial pressure of CO₂ in flue gas) and are not expected to be suitable for carbon capture under realistic conditions. We hypothesized that installation of a methoxy group in the HAT-3CN ring would achieve *in situ* incorporation of O-doped CO₂-philic sites on the surface of the material during the ZnCl₂-catalyzed high-temperature synthesis.^{34,35} In addition to the intrinsic N-doped moieties, we expected these O-dopants would thus significantly enhance the CO₂ affinities of the resultant adsorbents (HAT-CTFs, [Scheme 1](#)).

We first studied the polymerization of HAT-3CN at 400 °C via a well-developed ionothermal technique.³² As evidenced by the solid state ¹³C NMR ([Figure S1](#)), the trimerization of HAT-3CN can be confirmed by the existence of a triazine ring with a peak around 166 ppm.³⁶ The absence of any signal attributable to a methoxy group indicates complete decomposition of this functionality, putatively achieving *in situ* introduction of O-doped CO₂-philic sites into the final material. However, due to the nature of the synthesis and the modest ordering of the final material, the precise location of these sites in the chemical structure cannot be precisely determined from NMR. Residual nitrile groups (113 ppm) were also observed for HAT-CTF-400, suggesting a higher temperature is required to achieve complete trimerization. The N₂ adsorption isotherm of HAT-CTF-400 at 77 K was subsequently recorded to assess its Brunauer–Emmett–Teller (BET) surface area ([Figure S2](#)), which is

Received: July 24, 2016

Published: September 1, 2016

Scheme 1. Synthesis Route of Proposed O-Doped HAT-CTFs



much lower than expected ($17 \text{ m}^2 \text{ g}^{-1}$). This may be attributed to the planar structure of the HAT-based scaffold. However, to our delight, the CO_2 isotherm measured at 273 K reveals a permanent CO_2 uptake of 2.7 mmol g^{-1} (Figure 1a). Such

enhanced (Table 1). We attribute this to the partial carbonization of the material,²⁹ supported by the solid state ^{13}C NMR spectrum

Table 1. Comparison of Structural Parameters and CO_2 Capture Performance of HAT-CTFs with Other High-Performing Porous Adsorbents

sample	S_{BET} ($\text{m}^2 \text{ g}^{-1}$)	temperature (K)	CO_2 uptake (mmol g^{-1})	
			0.15 bar	1 bar
HAT-CTF-400	17	273	1.9	2.7
HAT-CTF-450	756	273	2.8	4.4
HAT-CTF-600	899	273	3.0	5.1
HAT-CTF-450/600	1090	273	3.0	6.3
		297	2.0	4.8
PPF-1 ^a	1740	273		6.1
		295		3.35
bipy-CTF600 ^b	2479	273		5.6
SU-MAC-500 ^c	941	273		6.03
		298		4.5

^aReported in ref 38. ^bReported in ref 31. ^cReported in ref 10.

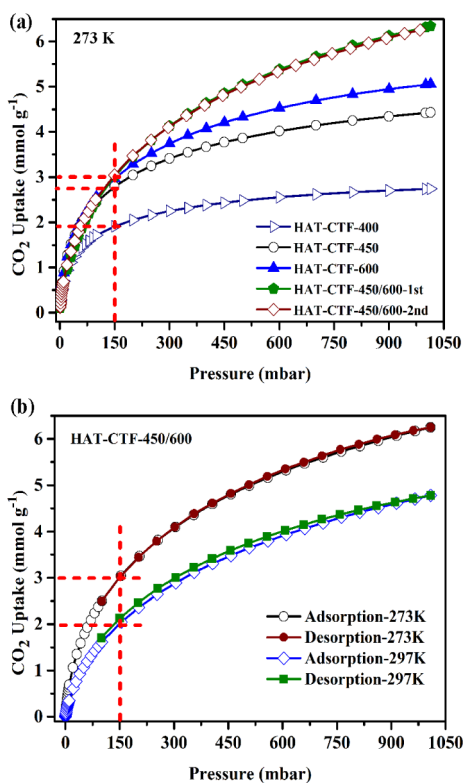


Figure 1. CO_2 uptake of HAT-CTFs at 273 K and 1 bar (a) and CO_2 adsorption–desorption of HAT-CTF-450/600 at both 273 and 297 K. Red lines were used to highlight the uptake at 0.15 bar.

counterintuitive phenomena were also reported by Schröder et al. for a supramolecular organic framework derived CO_2 adsorbent. It was suggested that interactions between N_2 and the channel windows of the framework at 77 K may hinder the diffusion of N_2 into the material, resulting in the modest specific surface area.³⁷

Trimerization reactions at higher temperatures were subsequently performed in an effort to enhance the BET surface areas of the resulting HAT-CTFs. As the synthesis temperature increased, the corresponding BET surface area was also

of HAT-CTF-450/600 (prepared at 450 °C for initial 20 h and another 20 h at 600 °C), where weak and broad signals around ~ 151 and 137 ppm from aromatic carbons in HAT ring were observed. The characteristic peak from the triazine ring disappeared during this process, similar to previously reported CTFs prepared at 600 °C.²⁹ The resulting new materials display Type I adsorption profiles (Figure S2). Notably, the amorphous framework HAT-CTF-450/600 (Figure S3) also possesses the largest BET surface area of $1090 \text{ m}^2 \text{ g}^{-1}$. The existence of “ultranano-pores,” extensive subnanometer ($<0.6 \text{ nm}$) material porosity, was demonstrated by a CO_2 isotherm at 273 K and analyzed by density functional theory modeling (Figure S4). The pore volume estimated from the CO_2 isotherm is $0.263 \text{ cm}^3 \text{ g}^{-1}$ at $P/P_0 = 0.99$, suggesting vast potential for the application of HAT-CTF-450/600 in CO_2 capture.

The CO_2 adsorption performance of HAT-CTFs were assessed by CO_2 isotherms performed at several different temperatures and 1 bar, revealing CO_2 uptake to be correlated with BET surface area. For example, HAT-CTF-600 ($S_{\text{BET}} = 899 \text{ m}^2 \text{ g}^{-1}$) exhibits a better CO_2 adsorption (5.1 mmol g^{-1}) than that of HAT-CTF-450 ($S_{\text{BET}} = 756 \text{ m}^2 \text{ g}^{-1}$, CO_2 uptake = 4.4 mmol g^{-1}). Despite HAT-CTF-450/600 displaying a specific BET surface area lower than that of many previously reported CTFs (determined through N_2 adsorption isotherms),³¹ an

exceptionally high CO₂ uptake of 6.3 mmol g⁻¹ was achieved (Figure 1a). This represents the highest CO₂ capacity for all POP-based adsorbents reported in the literature, as summarized in Table 1 and Table S1.^{31,38} For example, Zhang et al. reported a porous polymer framework (PPF-1, S_{BET} = 1740 m² g⁻¹) with a CO₂ capacity at 1 bar of 6.07 mmol g⁻¹ at 273 K and 3.35 mmol g⁻¹ at 295 K,³⁸ while the best CTF-based adsorbent (bipy-CTF600, S_{BET} = 2479 m² g⁻¹) was previously reported by Lotsch et al. and adsorbs 5.58 mmol g⁻¹ CO₂ at 273 K and 1 bar.³¹ Therefore, to the best of our knowledge, HAT-CTF-450/600 is the best POP-based adsorbent reported for carbon capture to date. More importantly, at 0.15 bar/273 K, HAT-CTF-450/600 adsorbs 3.0 mmol g⁻¹ CO₂, while at 297 K, this capacity decreases only modestly to 2.0 mmol g⁻¹, remaining significantly higher than that of a promising perfluorinated CTF-based adsorbent.³⁰ It should be noted that the adsorption of CO₂ at ~0.15 bar is more relevant to realistic carbon capture since flue gas contains approximately 15% CO₂ at total pressures of around 1 bar.²⁰ This CO₂ uptake achieved at 297 K and 1 bar (4.8 mmol g⁻¹, Figure 1b) also surpasses that of the polyamine-tethered porous polymer networks (4.3 mmol g⁻¹, 295 K, and 1 bar), which were previously the best POP-based adsorbents in the open literature.¹⁹ On account of the partial carbonization within the framework HAT-CTF-450/600, we also compared the CO₂ storage performance with N-doped carbonaceous adsorbents, which often exhibit better CO₂ uptake than that of POP-based materials. Very recently, Bao et al. reported a N-doped carbon adsorbent (SU-MAC-500, S_{BET} = 941 m² g⁻¹) with an impressive CO₂ uptake of 6.03 mmol g⁻¹ at 273 K and 1 bar, which is among the best of physisorptive micro- and mesoporous carbons.¹⁰ The CO₂ capture capacities of HAT-CTF-450/600 at either low or moderate pressure are superior to those of SU-MAC-500.

We propose that the synergistic effects of ultrananoporosity and abundant CO₂-philic surface sites play crucial roles in achieving this superior CO₂ capture performance. However, to provide a better understanding of the CO₂ adsorption in HAT-CTF-450/600, we have also calculated the isosteric heats of adsorption (Q_{st}) by fitting the CO₂ adsorption isotherms at 273 and 297 K and applying a variant of the Clausius–Clapeyron equation.³⁹ Q_{st} at low adsorption values was calculated to be 27.1 kJ mol⁻¹ (Figure S5), suggesting a strong dipole–quadrupole interaction between the polarizable CO₂ molecules and framework HAT-CTF-450/600.³⁶ Pragmatically, this means the CO₂ sorption isotherms of HAT-CTF-450/600 are effectively reversible (Figure 1b), affording a lower regeneration cost compared with conventional amine solutions.¹⁹ Excellent reuse of HAT-CTF-450/600 was demonstrated over five cycles of CO₂ adsorption at ~0.15 bar, confirming the electrostatic interaction partially responsible for CO₂ uptake is sufficiently weak to allow a facile regeneration of adsorbent (Figure S6).

We performed X-ray photoelectron spectroscopy (XPS) to study the active CO₂-philic sites on the surface of HAT-CTF-450/600 in an effort to gain deeper insight into the interaction between the framework and CO₂ (Figure 2). Previous work has shown that the surface functionalities of the adsorbents have a profound effect on the low-pressure adsorption, where the uptake depends less on the BET surface area than on adsorbent–CO₂ interactions.³⁰ This is clearly evident when comparing HAT-CTF-450/600 to the bipy-CTF600 reported by Lotsch et al.³¹ Despite possessing a significantly larger BET surface area than that of HAT-CTF-450/600 (2479 vs 1090 m² g⁻¹), better CO₂ uptake was obtained for our framework (5.6 vs 6.3 mmol g⁻¹ of CO₂ at 273 K and 1 bar). We reasoned that N/O codoping

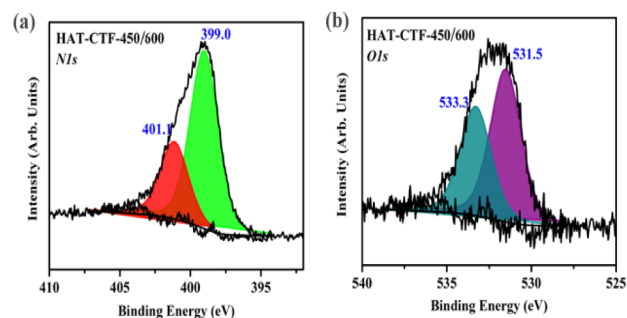


Figure 2. N 1s (a) and O 1s (b) XPS spectra of HAT-CTF-450/600.

could play an important role in carbon capture, and as anticipated, exceptionally high N-doping (32.8 at %) was achieved as a result of the N-rich HAT precursor. Pyridinic (399.0 eV, 68.9%) and pyrrolic nitrogen (401.1 eV, 31.1%) were the two different nitrogen species identified by XPS. These may serve as the binding sites for CO₂ uptake through electrostatic interaction,³¹ as the incorporation of more N-containing sites in POPs has previously been demonstrated to improve CO₂ adsorption capacities. Additionally, we also successfully obtained a high O-doping content of 9.4 at. %. The binding energy of O 1s at 531.5 eV was assigned to O=C (58.2%) and at 533.3 eV to O–C (41.8%), with further support from analysis of the C 1s orbital (Figure S7). We believe these rich O-doped sites help to enhance the affinity of the material surface for CO₂ and facilitate HAT-CTF-450/600–CO₂ uptake.

The *in situ* incorporation of additional O-doped sites on the surface of HAT-CTF-450/600 not only affected enhanced CO₂ uptake capacity but also afforded more preferential adsorption of CO₂ over N₂, i.e., higher CO₂/N₂ selectivity, another key factor for realistic carbon capture. The CO₂/N₂ selectivity for HAT-CTF-450/600 was calculated to be 160 at 273 K by the ratio of the initial slopes of CO₂ and N₂ adsorption isotherms (Figures S8 and S9). A value of 126 was achieved at 297 K, ranking HAT-CTF-450/600 among the most selective POP-based adsorbents (Table S1). CO₂/N₂ selectivity was also predicted using the ideal adsorption solution theory (IAST).^{39,40} Under simulated flue gas streams (typically 15% CO₂ and 85% N₂), HAT-CTF-450/600 exhibits high CO₂/N₂ selectivities at 1 bar (183 at 273 K and 110 at 297 K, Figure S10), which match well with those obtained from the initial slope method. This promising CO₂/N₂ selectivity further highlights the synergistic effects of ultrananoporosity and rich N/O codoped CO₂-philic sites within the polymeric architecture. As such, given the exceptionally high CO₂ uptake capacity and the intrinsic high thermal stability, this material may have potential for practical application in a postcombustion CO₂ capture.

In summary, an *in situ* doping strategy has been developed for the generation of a novel family of porous HAT-CTF-based adsorbents for efficient CO₂ capture. Significantly, at 297 K, HAT-CTF-450/600 can adsorb 4.8 mmol g⁻¹ of CO₂ at 1 bar (2.0 mmol g⁻¹ at 0.15 bar) due to the synergistic effects of ultrananopores and abundant N/O codoped CO₂-philic sites. This impressive result bestows HAT-CTF-450/600 with the highest CO₂ uptake capacity among known POPs. This innovative approach not only enables us to achieve an exceptionally high CO₂ uptake but also provides a means to control surface features of POPs and may open up new possibilities for the rational design and synthesis of new nanoporous materials for carbon capture.

■ ASSOCIATED CONTENT**■ Supporting Information**

The Supporting Information is available free of charge on the ACS Publications website at DOI: [10.1021/jacs.6b07644](https://doi.org/10.1021/jacs.6b07644).

Experimental section, Figures S1–12, and Table S1 (PDF)

■ AUTHOR INFORMATION**Corresponding Authors**

*tianchengcheng.ecust@gmail.com

*dais@ornl.gov

Notes

The authors declare no competing financial interest.

■ ACKNOWLEDGMENTS

The research was supported financially by the Division of Chemical Sciences, Geosciences, and Biosciences, Office of Basic Energy Sciences, US Department of Energy.

■ REFERENCES

- (1) D'Alessandro, D. M.; Smit, B.; Long, J. R. *Angew. Chem., Int. Ed.* **2010**, *49*, 6058.
- (2) Nugent, P.; Belmabkhout, Y.; Burd, S. D.; Cairns, A. J.; Luebke, R.; Forrest, K.; Pham, T.; Ma, S.; Space, B.; Wojtas, L.; Eddaoudi, M.; Zaworotko, M. J. *Nature* **2013**, *495*, 80.
- (3) Li, D.; Furukawa, H.; Deng, H.; Liu, C.; Yaghi, O. M.; Eisenberg, D. S. *Proc. Natl. Acad. Sci. U. S. A.* **2014**, *111*, 191.
- (4) Zhang, Z.; Yao, Z.-Z.; Xiang, S.; Chen, B. *Energy Environ. Sci.* **2014**, *7*, 2868.
- (5) Fracaroli, A. M.; Furukawa, H.; Suzuki, M.; Dodd, M.; Okajima, S.; Gándara, F.; Reimer, J. A.; Yaghi, O. M. *J. Am. Chem. Soc.* **2014**, *136*, 8863.
- (6) Datta, S. J.; Khumnoon, C.; Lee, Z. H.; Moon, W. K.; Docao, S.; Nguyen, T. H.; Hwang, I. C.; Moon, D.; Oleynikov, P.; Terasaki, O.; Yoon, K. B. *Science* **2015**, *350*, 302.
- (7) McDonald, T. M.; Mason, J. A.; Kong, X.; Bloch, E. D.; Gygi, D.; Dani, A.; Crocella, V.; Giordanino, F.; Odoh, S. O.; Drisdell, W. S.; Vlaisavljevich, B.; Dzubak, A. L.; Poloni, R.; Schnell, S. K.; Planas, N.; Lee, K.; Pascal, T.; Wan, L. F.; Prendergast, D.; Neaton, J. B.; Smit, B.; Kortright, J. B.; Gagliardi, L.; Bordiga, S.; Reimer, J. A.; Long, J. R. *Nature* **2015**, *519*, 303.
- (8) Zhao, X.; Bu, X.; Zhai, Q.-G.; Tran, H.; Feng, P. *J. Am. Chem. Soc.* **2015**, *137*, 1396.
- (9) Zhai, Q.-G.; Bu, X.; Mao, C.; Zhao, X.; Feng, P. *J. Am. Chem. Soc.* **2016**, *138*, 2524.
- (10) To, J. W. F.; He, J.; Mei, J.; Haghpanah, R.; Chen, Z.; Kurosawa, T.; Chen, S.; Bae, W.-G.; Pan, L.; Tok, J. B. H.; Wilcox, J.; Bao, Z. *J. Am. Chem. Soc.* **2016**, *138*, 1001.
- (11) Zeng, Y.; Zou, R.; Zhao, Y. *Adv. Mater.* **2016**, *28*, 2855.
- (12) Slater, A. G.; Cooper, A. I. *Science* **2015**, *348*, 988.
- (13) Dawson, R.; Adams, D. J.; Cooper, A. I. *Chem. Sci.* **2011**, *2*, 1173.
- (14) Dawson, R.; Stockel, E.; Holst, J. R.; Adams, D. J.; Cooper, A. I. *Energy Environ. Sci.* **2011**, *4*, 4239.
- (15) Rabbani, M. G.; El-Kaderi, H. M. *Chem. Mater.* **2011**, *23*, 1650.
- (16) Ben, T.; Li, Y.; Zhu, L.; Zhang, D.; Cao, D.; Xiang, Z.; Yao, X.; Qiu, S. *Energy Environ. Sci.* **2012**, *5*, 8370.
- (17) Chen, Q.; Luo, M.; Hammershøj, P.; Zhou, D.; Han, Y.; Laursen, B. W.; Yan, C.-G.; Han, B.-H. *J. Am. Chem. Soc.* **2012**, *134*, 6084.
- (18) Luo, Y.; Li, B.; Wang, W.; Wu, K.; Tan, B. *Adv. Mater.* **2012**, *24*, 5703.
- (19) Lu, W.; Yuan, D.; Sculley, J.; Zhao, D.; Krishna, R.; Zhou, H.-C. *J. Am. Chem. Soc.* **2011**, *133*, 18126.
- (20) Lu, W.; Sculley, J. P.; Yuan, D.; Krishna, R.; Wei, Z.; Zhou, H.-C. *Angew. Chem., Int. Ed.* **2012**, *51*, 7480.
- (21) Modak, A.; Nandi, M.; Mondal, J.; Bhaumik, A. *Chem. Commun.* **2012**, *48*, 248.
- (22) Lu, W.; Verdegaal, W. M.; Yu, J.; Balbuena, P. B.; Jeong, H.-K.; Zhou, H.-C. *Energy Environ. Sci.* **2013**, *6*, 3559.
- (23) Patel, H. A.; Hyun Je, S.; Park, J.; Chen, D. P.; Jung, Y.; Yavuz, C. T.; Coskun, A. *Nat. Commun.* **2013**, *4*, 1357.
- (24) Arab, P.; Rabbani, M. G.; Sekizkardes, A. K.; İslamoğlu, T.; El-Kaderi, H. M. *Chem. Mater.* **2014**, *26*, 1385.
- (25) Huang, N.; Chen, X.; Krishna, R.; Jiang, D. *Angew. Chem., Int. Ed.* **2015**, *54*, 2986.
- (26) Huang, N.; Krishna, R.; Jiang, D. *J. Am. Chem. Soc.* **2015**, *137*, 7079.
- (27) Stegbauer, L.; Hahn, M. W.; Jentys, A.; Savasci, G.; Ochsenfeld, C.; Lercher, J. A.; Lotsch, B. V. *Chem. Mater.* **2015**, *27*, 7874.
- (28) Xiang, Z.; Mercado, R.; Huck, J. M.; Wang, H.; Guo, Z.; Wang, W.; Cao, D.; Haranczyk, M.; Smit, B. *J. Am. Chem. Soc.* **2015**, *137*, 13301.
- (29) Chang, T.-H.; Wu, B.-R.; Chiang, M. Y.; Liao, S.-C.; Ong, C. W.; Hsu, H.-F.; Lin, S.-Y. *Org. Lett.* **2005**, *7*, 4075.
- (30) Zhao, Y.; Yao, K. X.; Teng, B.; Zhang, T.; Han, Y. *Energy Environ. Sci.* **2013**, *6*, 3684.
- (31) Hug, S.; Stegbauer, L.; Oh, H.; Hirscher, M.; Lotsch, B. V. *Chem. Mater.* **2015**, *27*, 8001.
- (32) Katekomol, P.; Roeser, J.; Bojdys, M.; Weber, J.; Thomas, A. *Chem. Mater.* **2013**, *25*, 1542.
- (33) Ren, S.; Bojdys, M. J.; Dawson, R.; Laybourn, A.; Khimyak, Y. Z.; Adams, D. J.; Cooper, A. I. *Adv. Mater.* **2012**, *24*, 2357.
- (34) Kuhn, P.; Antonietti, M.; Thomas, A. *Angew. Chem., Int. Ed.* **2008**, *47*, 3450.
- (35) Kuhn, P.; Forget, A.; Su, D.; Thomas, A.; Antonietti, M. *J. Am. Chem. Soc.* **2008**, *130*, 13333.
- (36) Zhu, X.; Tian, C.; Mahurin, S. M.; Chai, S.-H.; Wang, C.; Brown, S.; Veith, G. M.; Luo, H.; Liu, H.; Dai, S. *J. Am. Chem. Soc.* **2012**, *134*, 10478.
- (37) Lü, J.; Perez-Krap, C.; Suyetin, M.; Alsmail, N. H.; Yan, Y.; Yang, S.; Lewis, W.; Bichoutskaia, E.; Tang, C. C.; Blake, A. J.; Cao, R.; Schröder, M. *J. Am. Chem. Soc.* **2014**, *136*, 12828.
- (38) Zhu, Y.; Long, H.; Zhang, W. *Chem. Mater.* **2013**, *25*, 1630.
- (39) Zhu, X.; Mahurin, S. M.; An, S.-H.; Do-Thanh, C.-L.; Tian, C.; Li, Y.; Gill, L. W.; Hagaman, E. W.; Bian, Z.; Zhou, J.-H.; Hu, J.; Liu, H.; Dai, S. *Chem. Commun.* **2014**, *50*, 7933.
- (40) Zhao, Y.; Liu, X.; Han, Y. *RSC Adv.* **2015**, *5*, 30310.